

## ARTICLE

## Measurement of Proton-production Double Differential Cross Sections from 290 MeV/u $^{12}\text{C}$ Incidence on Carbon at Forward Angles

Yohei FUKUDA<sup>1</sup>, Kazuya TAHARA<sup>1</sup>, Genichiro WAKABAYASHI<sup>1\*</sup>, Hisashi BAN<sup>1</sup>, Yousuke MORIMOTO<sup>1</sup>,  
 Katashi KIYOHARA<sup>1</sup>, Yoshinori FUKUI<sup>1</sup>, Yusuke KOBAYASHI<sup>1</sup>, Hiroki IWAMOTO<sup>1</sup>, Minoru IMAMURA<sup>1</sup>,  
 Yusuke UOZUMI<sup>1</sup> and Naruhiro MATSUFUJI<sup>2</sup>

<sup>1</sup>Kyushu University, 744, Motoooka, Nishi-ku, Fukuoka 819-0395, Japan

<sup>2</sup>National Institute of Radiological Sciences, 4-1-9, Anagawa, Inage-ku, Chiba 263-8555, Japan

Proton-production double differential cross sections were investigated for the interaction of 290 MeV/u carbon beams with a carbon target. Measurements were carried out at forward angles from 3 to 15 degrees. A spectrometer used in the measurement consists of two plastic scintillators, four cubic GSO(Ce) crystals and one cylindrical GSO(Ce) crystal. The preliminary results on the double differential cross sections were reported and compared with PHITS code simulations.

**KEYWORDS:** heavy ion induced reactions, carbon beam, proton production double differential cross section, carbon target, GSO(Ce) detector

### I. Introduction

Recently, heavy ion induced reactions are of great interest in the field of medicine and engineering. In cancer therapy using heavy ion beams, light fragments such as hydrogen and helium produced are important because they have long ranges in a human body and give unwanted dose to normal tissues. To estimate the dose distribution including the effect of light fragments, the precise simulation code based on experimentally measured double differential cross section (DDX) data is needed. However, the existing data on light ion production interactions are insufficient to establish a reliable simulation code.

In this study, we measured the energy spectra of protons from the interactions of 290 MeV/u  $^{12}\text{C}$  with a graphite target at four forward angles. In the following sections, a spectrometer used in the measurement is described and an experimental procedure and an analytical method are reported. In addition, the preliminary results on DDXs are presented and compared with the calculations using the heavy ion transport code PHITS<sup>1)</sup>.

### II. Experiments

Experiments were performed at the heavy ion accelerator facility HIMAC (Heavy Ion Medical Accelerator in Chiba) of the National Institute of Radiological Sciences in Japan. The carbon beams of 290 MeV/u were delivered on a graphite target. The beam spot size was smaller than 5 mm in diameter and centered on the target. The beam intensity was about  $10^5$ - $10^6$  particles in each beam bunch at a cycle of 3.3 seconds. **Figure 1** shows the layout of the experimental setup. The number of incident particles was measured with a 1 mm thick plastic scintillator (Beam Monitor) that was located just behind the exit of the beam

line. The target used in the measurement was a 2 mm thick graphite plate with the density of  $1.82 \text{ g/cm}^3$ . The particles emitted from the nuclear reactions in the target were detected by a spectrometer placed at  $3^\circ$ ,  $5^\circ$ ,  $10^\circ$  and  $15^\circ$  with respect to the beam axis. Measurements were also carried out without the target to investigate background events.

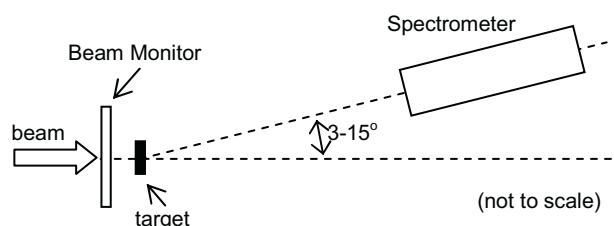


**Fig. 1** The layout of the experimental setup.

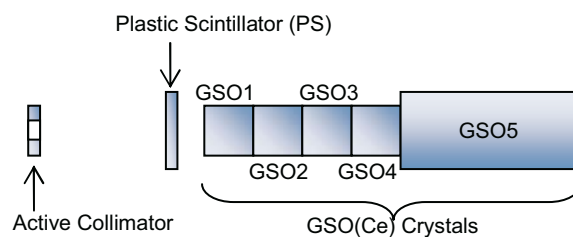


**Fig. 2** The configuration of the spectrometer.

**Figure 2** shows the configuration of the spectrometer used in the measurement. The spectrometer is stacked scintillators and consists of two plastic scintillators, four cubic GSO(Ce) crystals and one cylindrical GSO(Ce) crystal. We used multiple detectors in tandem as a spectrometer in order to apply the  $\Delta E$ -E method for particle identification in different energy regions. For instance, the protons with energy higher than 160 MeV and lower than 245 MeV pass through the first GSO(Ce) crystal and stop in the second GSO(Ce) crystal. Using the first GSO(Ce) crystal as a

\*Corresponding Author, E-mail: gensan@nucl.kyushu-u.ac.jp  
 © Atomic Energy Society of Japan

transmission detector ( $\Delta E$ ) and the second one as a stop detector ( $E$ ), the  $\Delta E$ - $E$  method can be applied for particle identification in the above energy region. Furthermore, the protons with the energy higher than 245 MeV and lower than 310 MeV pass through the first and second GSO(Ce) crystals and stop in the third GSO(Ce) crystal. Again, the same procedure can be used for particle identification in the next energy region. In this way, particle identification was carried out in different energy regions combining neighboring detectors as  $\Delta E$  and  $E$  detectors.

The active collimator (Fig. 2) is a 10 mm thick plastic scintillator with a circular aperture of 15 mm in diameter at the center. This defines the solid angle of the measurement and cuts off the events that produce any signal in this detector. The thickness of the plastic scintillator (PS in Fig. 2) is 10 mm. The cubic GSO(Ce) crystal is 43 mm thick and the cylindrical one is 120 mm thick. The total depth of the GSO(Ce) crystals is 292 mm, which is thick enough to stop protons up to 500 MeV. From upper stream we call the GSO(Ce) crystals GSO1 to GSO5 in sequence. One side of each scintillator was optically coupled to a photomultiplier tube (PMT), and each scintillator was wrapped with an aluminum foil for light reflection and black plastic tapes for light shielding.

The signals from the detectors were processed in a standard electronic setup of NIM and CAMAC modules. The output charges from the PMTs were digitized with a CAMAC ADC and recorded event-by-event on the hard disk of a PC. The coincidence signal between the beam monitor, PS and GSO1 detectors was used as a trigger to open the ADC gate.

### III. Analysis

#### 1. Energy Calibration

The relationships between the energy deposition and the light output of plastic scintillators and GSO(Ce) crystals were obtained by using the Bethe-Bloch equation<sup>2)</sup> and the Birks equation<sup>3)</sup>. The Bethe-Bloch equation is a semiempirical formula to calculate energy loss per unit length (stopping power), and is given as,

$$\frac{dE}{dx} = 4\pi r_0^2 z^2 \frac{mc^2}{\beta^2} NZ \left[ \ln \left( \frac{2mc^2 \beta^2}{I} \right) - \ln(1 - \beta^2) - \beta^2 \right], \quad (1)$$

where  $r_0$  is the classical electron radius,  $z$  the charge of the incident particle,  $mc^2$  the electron rest mass energy,  $\beta = v/c$ ,  $N$  the number of atoms in the target material,  $Z$  the atomic number of the material.

The Birks equation gives light output per unit length using stopping power, and is defined by,

$$\frac{dL}{dx} = \frac{S \left( \frac{dE}{dx} \right)}{1 + kB \left( \frac{dE}{dx} \right)}, \quad (2)$$

or one can write in the following way by taking a higher order term,

$$\frac{dL}{dx} = \frac{S \left( \frac{dE}{dx} \right)}{1 + kB \left( \frac{dE}{dx} \right) + \eta \left( kB \frac{dE}{dx} \right)^2}, \quad (3)$$

where  $S$  is the scintillation factor,  $kB$  the so called Birks parameter that relates to scintillation quenching and  $\eta$  the arbitrary constant. We used eq. (2) for the plastic scintillator and (3) for the GSO(Ce) crystals because of the high stopping power of a GSO(Ce) crystal. The values of  $kB$  have been determined to be  $1.29 \times 10^{-5}$  m/MeV for plastic scintillators and  $0.57 \times 10^{-5}$  m/MeV for GSO(Ce) crystals, respectively<sup>4)</sup>. The values of  $S$  were determined as arbitrary constants in the analytical procedure because the light outputs from the detectors were recorded as ADC channels.

The light output from each detector was converted to the energy deposition in the following way. First, we placed the spectrometer on the beam axis and measured the light output for 290 MeV/u carbon beams. The carbon beams penetrate the plastic scintillator (PS) and fully stop in the first GSO(Ce) crystal (GSO1), and the light outputs corresponding to the energy depositions of carbon beams in PS and GSO1 detectors were measured. Using the measured results and eqs. (1) and (2) or (3), the relationships between the energy deposition and the light output for carbon beams were determined for PS and GSO1. Next the  $\gamma$ -rays from a <sup>137</sup>Cs source were irradiated to all the GSO(Ce) crystals to measure the ratio of the light outputs from the rest of the GSO(Ce) crystals (GSO2-5) to that from GSO1. Thus the relationships between the energy deposition and the light output for carbon beams were determined for all the GSO(Ce) crystals by using the ratio of the light outputs for <sup>137</sup>Cs. Because the ratio of the light output for carbon beams to that for protons has been investigated in previous studies<sup>5,6)</sup>, the relationship between the energy deposition and the light output for protons were finally determined for all the detectors.

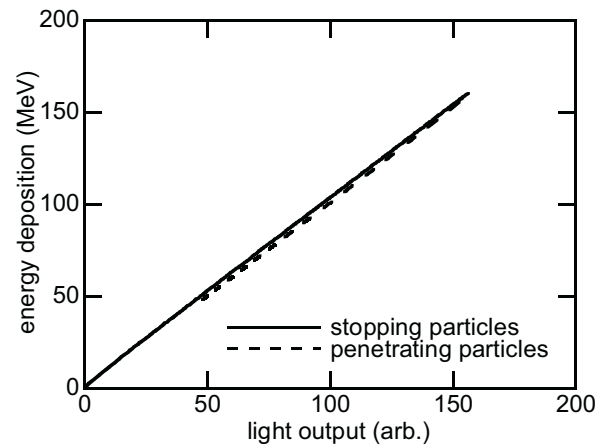
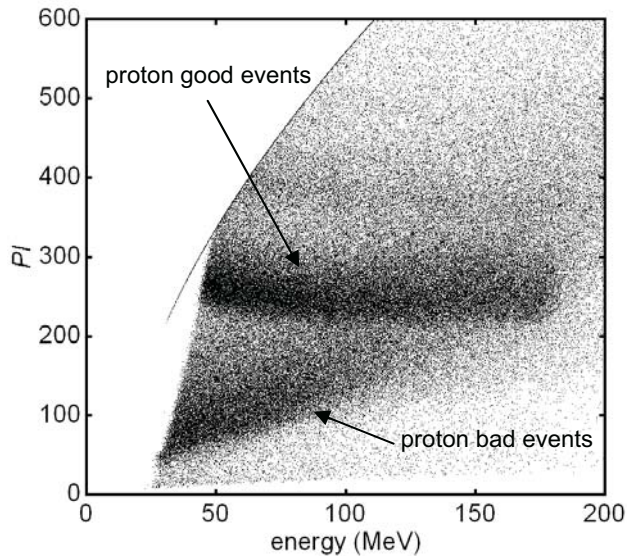


Fig. 3 The relationship between the energy deposition and the light output in a GSO(Ce) crystal ( $43 \times 43 \times 43$  mm<sup>3</sup>) for protons.

Figure 3 shows an example of the relationship between the energy deposition and the light output for protons. Note

that the light output for protons is slightly different between the cases for stopping protons and penetrating protons.



**Fig. 4** The two dimensional plot of  $PI$  versus proton energy. The thick belt lying around  $PI \sim 250$  corresponds to proton good events.

## 2. Particle Identification

As mentioned in Section II, particle identification was carried out by the  $\Delta E$ - $E$  method. In this study, we used the parameter,  $PI$ , which is defined by<sup>7)</sup>,

$$PI = E_{total}^b - (E_{total} - \Delta E)^b, \quad (4)$$

where  $b$  is the parameter representing the range of each particle,  $E_{total}$  the total energy deposited in the spectrometer, and  $\Delta E$  the amount of energy deposited in the transmission detector. A value of 1.73 was employed for the parameter  $b$ <sup>8)</sup>. In **Fig. 4**, a typical two-dimensional plot of  $PI$  versus particle energy is shown for PS and GSO1 detectors. The thick belt lying around  $PI \sim 250$  corresponds to proton good events, which are due to the protons stopped in the crystal GSO1 through electronic interactions. The lower area is a group of proton bad events, which are the events that did not provide full energy to the crystal because of nuclear reactions in the crystal or scattering out of the crystal volume.

## IV. Results

Double differential cross sections were obtained in the following way. First, a  $PI$  projection spectrum was generated for each energy bin of 20 MeV width. **Figure 5** shows a typical projection spectrum for the energy range from 80 to 100 MeV. We separated proton good events in the projection spectra and counted the number of events in the peak.

Next, DDXs were determined by the following equation,

$$DDX = \frac{Y}{N_b \cdot N_t \cdot E_b \cdot \Omega \cdot \varepsilon_p \cdot \varepsilon_D}, \quad (5)$$

where  $Y$  is the number of proton events in an energy bin,  $N_b$  the number of incident ions on the target,  $N_t$  the number of atoms in the target ( $\text{cm}^2$ ),  $E_b$  the width of an energy bin,  $\Omega$

the solid angle seen by the spectrometer,  $\varepsilon_p$  the peak efficiency,  $\varepsilon_D$  the DAQ efficiency.

The peak efficiency is defined as the ratio of the number of proton good events to the total number of proton events. In the present work, the peak efficiency was determined as a function of proton energy by the simulations with the PHITS code. **Figure 6** shows the simulated peak efficiency used for the correction. The DAQ efficiency is an efficiency which corrects for the effect of dead time in the CAMAC-PC data acquisition system.

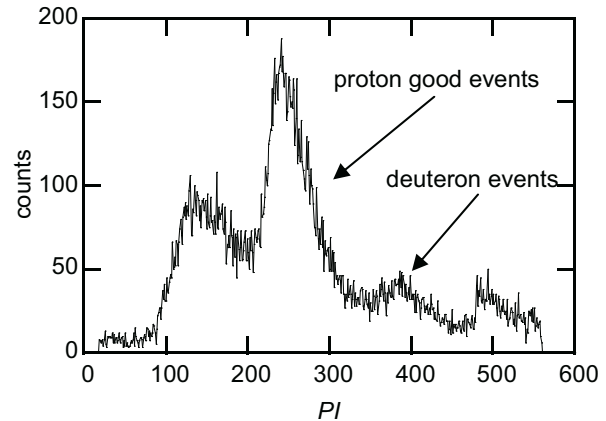


**Fig. 5** A typical projection spectrum for the energy bin of 20 MeV width. This example shows the spectrum for the energy range from 80 to 100 MeV.

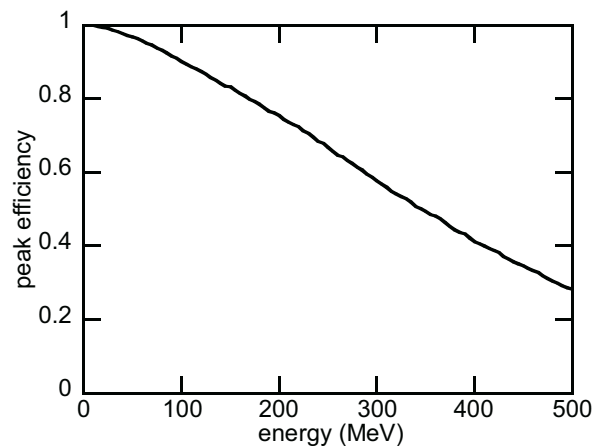


**Fig. 6** The peak efficiency of a GSO(Ce) crystal ( $43 \times 43 \times 43 \text{ mm}^3$ ) for protons.

The contributions of background events were determined by the experiment without the sample above and subtracted from the data for the measurement with the target.

The preliminary results on the DDXs are shown in **Fig. 7**. The measured results are shown with the calculated results with the PHITS code. The experimental results show good agreement with the simulation at  $3^\circ$  except for the energy region below 160 MeV. However, the experimental data below 160 MeV should be checked further because they may still include proton bad events or noise events. The experimental data at  $5^\circ$  and  $10^\circ$  agree well with the simulation up to around 250 MeV but show some

disagreement in higher energy region. On the other hand, the experimental results at  $15^\circ$  disagree with the simulation over the whole energy region: the PHITS simulation overestimates the experimental DDX.

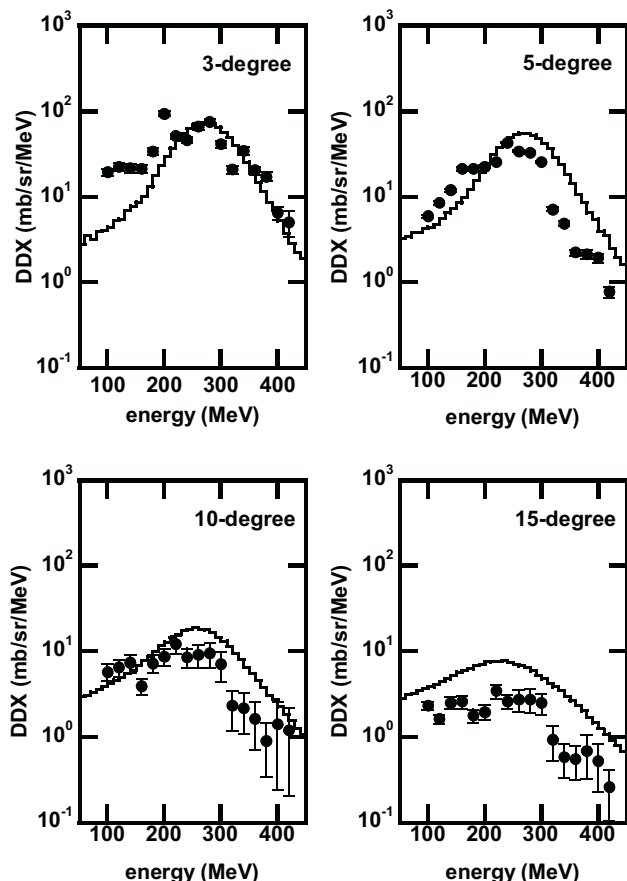


Fig. 7 The preliminary results on proton production double differential cross sections for carbon-carbon reaction at four forward angles.

## V. Conclusions

The proton-production double differential cross sections for 290 MeV/u  $^{12}\text{C}$  incidence on a graphite target were

measured at four different forward angles. The spectrometer used in the measurement was stacked scintillators that consisted of plastic scintillators and GSO(Ce) crystals. The measured DDXs were compared with the PHITS simulation. The experimental results generally agreed with the simulation but had some disagreement. In order to understand the observed discrepancies, more detailed analysis and further measurements are needed.

## Acknowledgment

The experiment was carried out under the Research Project with Heavy Ions at NIRS-HIMAC, program 18P214. This work was partially supported by the Ministry of Education, Science, Sports and Culture, Grant-in-Aid for Young Scientists (B), 17760682, 2005-2007.

## References

- 1) H. Iwase, K. Niita, T. Nakamura, "Development of general-purpose particle and heavy ion transport Monte Carlo code", *J. Nucl. Sci. Technol.*, 39[11], 1142 (2002).
- 2) N. Tsoulfanidis, *Measurement and Detection of Radiation*, Second Edition, Taylor & Francis, 124 (1995).
- 3) J. B. Birks, *The theory and practice of scintillation counting*, Pergamon Press, (1964).
- 4) M. Imamura, Y. Yamashita, P. Evtoukhoviich, et al., "Response characteristics of GSO(Ce) crystal to intermediate-energy  $\alpha$ -particles", *Nucl. Instrum. Methods*, A564, 324 (2006).
- 5) H. Yoshida, D. Konishi, K. Anami, et al., "Absolute efficiency of a stacked GSO(Ce) spectrometer for intermediate energy protons", *Nucl. Instrum. Methods*, A411[1], 46 (1998).
- 6) G. Wakabayashi, Y. Koba, M. Imamura, et al., "Light output response of GSO(Ce) crystals to relativistic carbon ions", *Nuclear Science Symposium Conference Record*, IEEE 2006, 2 1175 (2006).
- 7) M. Makino, R. Eisburg, D. Ingham, C. Waddell, "A method for reducing the effect of nuclear reaction in stopping detectors", *Nucl. Instrum. Methods*, 81, 125 (1970).
- 8) T. Kin, F. Saiho, S. Hohara, et al., "Proton production cross sections for reactions by 300- and 392-MeV protons on carbon, aluminum, and niobium", *Phys. Rev. C*72, 014606 (2005).